Clinical Neurophysiology 131 (2020) 2795–2803

Contents lists available at ScienceDirect

Clinical Neurophysiology

journal homepage: www.elsevier.com/locate/clinph

High-density Electric Source Imaging of interictal epileptic discharges: How many electrodes and which time point?

Bernd J. Vorderwülbecke [a,b,1], Margherita Carboni [a,c,1], Sebastien Tourbier [d], Denis Brunet [c], Martin Seeber [c], Laurent Spinelli [a], Margitta Seeck [a], Serge Vulliemoz [a,*]

[a] EEG and Epilepsy Unit, University Hospitals and Faculty of Medicine, University of Geneva, Rue Gabrielle-Perret-Gentil 4, 1205 Geneva, Switzerland
[b] Department of Neurology, Epilepsy-Center Berlin-Brandenburg, Charité – Universitätsmedizin Berlin, Charitéplatz 1, 10117 Berlin, Germany
[c] Functional Brain Mapping Lab, Department of Basic Neurosciences, University of Geneva, Campus Biotech, 9 Chemin des Mines, 1202 Geneva, Switzerland
[d] Connectomics Lab, Department of Radiology, Lausanne University Hospital, Rue du Bugnon 46, 1011 Lausanne, Switzerland

ARTICLE INFO

Article history:
Accepted 7 September 2020
Available online 15 October 2020

Keywords:
EEG source localization
Focal epilepsy
Epilepsy surgery
Locally spherical model with anatomical constraints
Local autoregressive average

HIGHLIGHTS

- Down-sampling of 257- to 204-channel EEG by removing cheek and neck electrodes can improve accuracy of EEG source localisation.
- This may be due to both higher artefact load in caudal channels and insufficient biophysical modelling of inferior head areas.
- In comparison to earlier time points or the spike peak, 50% of the averaged spike's rising phase provided most accurate results.

ABSTRACT

Objective: To assess the value of caudal EEG electrodes over cheeks and neck for high-density electric source imaging (ESI) in presurgical epilepsy evaluation, and to identify the best time point during averaged interictal epileptic discharges (IEDs) for optimal ESI accuracy.
Methods: We retrospectively examined presurgical 257-channel EEG recordings of 45 patients with pharmacoresistant focal epilepsy. By stepwise removal of cheek and neck electrodes, averaged IEDs were downsampled to 219, 204, and 156 EEG channels. Additionally, ESI at the IED's half-rise was compared to other time points. The respective sources of maximum activity were compared to the resected brain area and postsurgical outcome.
Results: Caudal channels had disproportionately more artefacts. In 30 patients with favourable outcome, the 204-channel array yielded the most accurate results with ESI maxima < 10 mm from the resection in 67% and inside affected sublobes in 83%. Neither in temporal nor in extratemporal cases did the full 257-channel setup improve ESI accuracy. ESI was most accurate at 50% of the IED's rising phase.
Conclusion: Information from cheeks and neck electrodes did not improve high-density ESI accuracy, probably due to higher artefact load and suboptimal biophysical modelling.
Significance: Very caudal EEG electrodes should be used for ESI with caution.
© 2020 International Federation of Clinical Neurophysiology. Published by Elsevier B.V. This is an open access article under the CC BY license (http://creativecommons.org/licenses/by/4.0/).

1. Introduction

In patients with pharmacoresistant focal epilepsy, epilepsy surgery aims at eliminating the epileptogenic zone, *i.e.* the specific area of cerebral cortex which is indispensable for the generation of seizures. A valuable, non-invasive neurophysiological tool to approach the epileptogenic zone is electric source imaging (ESI). Based on the patient's scalp electroencephalogram (EEG), ESI plots the sources of epileptic activity within a 3D model of the patient's brain (Zijlmans et al., 2019; Foged et al., 2020). ESI can be applied

Abbreviations: ESI, electric source imaging; IED, interictal epileptic discharge; IQR, interquartile range; ILAE, international league against epilepsy; LSMAC, locally spherical model with anatomical constraints.

* Corresponding author at: EEG and Epilepsy Unit, University Hospitals Geneva, Rue Gabrielle-Perret-Gentil 4, 1205 Geneva, Switzerland.
E-mail addresses: bernd.vorderwuelbecke@charite.de (B.J. Vorderwülbecke), margherita.carboni01@gmail.com (M. Carboni), sebastien.tourbier@alumni.epfl.ch (S. Tourbier), denis.brunet@unige.ch (D. Brunet), martin.seeber@unige.ch (M. Seeber), laurent.spinelli@hcuge.ch (L. Spinelli), margitta.seeck@hcuge.ch (M. Seeck), serge.vulliemoz@hcuge.ch (S. Vulliemoz).
[1] Contributing equally.

https://doi.org/10.1016/j.clinph.2020.09.018
1388-2457/© 2020 International Federation of Clinical Neurophysiology. Published by Elsevier B.V.
This is an open access article under the CC BY license (http://creativecommons.org/licenses/by/4.0/).

on both ictal (Beniczky et al., 2016; Nemtsas et al., 2017) and interictal epileptic discharges (IEDs). IEDs occur more frequently than ictal EEG patterns and are less often corrupted by movement artefacts. They display relatively simple spatio-temporal dynamics and can easily be averaged to achieve a high signal-to-noise ratio (Pittau et al., 2014). In comparison to spherical head models and standard EEG with up to 32 electrodes, accuracy of ESI was found to increase with the use of individual realistic head models and high-density EEG with up to 257 electrodes (Lantz et al., 2003a; Brodbeck et al., 2011; Foged et al., 2020).

While the standard EEG array recommended by the International Federation of Clinical Neurophysiology (IFCN) covers the neurocranium above the hat brim line plus 6 electrodes in the inferior temporal chain, modern high-density EEG setups offer a much more caudal head coverage, including face and neck (Seeck et al., 2017). Simulated data indicate a substantial increase in ESI accuracy if regions below the hat brim line are covered (Song et al., 2015). However, the additional value of inferior electrodes for ESI has never been assessed empirically in patients with epilepsy. On the one hand, due to their spatial proximity to the skull base, caudal EEG channels may help in localizing epileptic activity in basal structures such as the temporal lobes. On the other hand, located rather far from the convexity, they might be of less value for ESI in most extratemporal structures. In addition, caudal electrodes placed on face and neck record signals after complex propagation through several types of tissue and air (sinus cavities) and are relatively prone to muscle artefacts. These effects lower the signal quality recorded at these sites and may, in turn, reduce these electrodes' value for ESI.

At the EEG and Epilepsy Unit of the University Hospitals Geneva, ESI for clinical and scientific use is currently based on 257-channel EEG down-sampled to 204 channels and has been validated with this approach (Birot et al., 2014; Staljanssens et al., 2017). To eliminate the contribution of electrodes most affected by artefacts, the 204-channel setup does not include the most caudal row of electrodes covering the neck, nor does it cover the cheeks. In order to provide a reference for future clinical work, we aimed at evaluating this "default" methodology by comparing its results to those achieved with 257, 219 or 156 EEG channels. We hypothesised that ESI based on the full 257-electrode setup would be superior to 204 channels in temporal lobe epilepsy but not in extratemporal epilepsy. We further expected an "intermediate" 219-channel setup that includes inferior temporal electrodes to yield balanced results, and a very reduced 156-channel array above the hat brim line to perform rather poorly (Fig. 1 A, Supplementary Fig. 1).

ESI is commonly performed at single time points, based on the respective EEG scalp voltage map at those specific moments in time. Thanks to the high temporal resolution of EEG in the order of milliseconds, different time points across an IED can be evaluated. The IED peak offers the highest signal-to-noise ratio; however, its source estimation may already be subject to propagation (Merlet et al., 1997; Lantz et al., 2003b; Bast et al., 2006; Plummer et al., 2010). Therefore, interictal ESI is most often performed at 50% of the IED's rising phase (Brodbeck et al., 2011; Megevand et al., 2014; Feng et al., 2016; Centeno et al., 2017). Still, some authors report highest ESI accuracy at very early time points of the IED (Plummer et al., 2019) or, on the contrary, at the IED peak (van Mierlo et al., 2017). Thus, we additionally compared ESI accuracy at five different time points along the IED's rising slope.

2. Patients and methods

2.1. Patient recruitment

Until July 31st, 2019, the database of the EEG and Epilepsy Unit at the University Hospitals Geneva was retrospectively screened for patients meeting the following criteria: (a) a first resective brain surgery to treat pharmacoresistant focal epilepsy; (b) age older than 6 years at evaluation; (c) presurgical 257-channel EEG recording with a minimum of 3 focal IEDs; (d) presurgical high-resolution magnetic resonance imaging (MRI); (e) known 12-month postsurgical outcome. According to the International League Against Epilepsy (ILAE) criteria (Wieser et al., 2001), patients were classified as having favourable 12-month postsurgical outcome (ILAE 1 + 2: seizure-free or "auras" only since surgery, equivalent to Engel IA and IB) or rather unfavourable outcome (ILAE 3 or higher: not seizure-free). The study was approved by the local ethics committee at the University Hospitals Geneva.

2.2. EEG acquisition and pre-processing

High-density EEG recordings (257 electrodes; unfiltered acquisition, sampling rate 500–1000 Hz) were acquired during presurgical epilepsy evaluation at the University Hospitals Geneva (EGI Philips / Magstim EGI, Eugene, US-OR). For clinical purposes, an EEG experienced neurologist (M. Seeck, S. Vulliemoz, and others) visually identified interictal spikes (<70 ms) and sharp waves (70–200 ms) using conventional display (*e.g.*, longitudinal bipolar or average reference montages of the 10–20 electrode array plus 6 electrodes in the inferior temporal chain, corresponding to the 2017 IFCN recommendations (Seeck et al., 2017)). In order to avoid any possible propagation/interference effects, IEDs occurring earlier than 1 second after a previous IED were not considered. IEDs of the same configuration and localisation were considered homologous. In the current study, 8 individuals had more than one type of homologous IEDs, and we used that IED type which occurred most often or, if the number of single IEDs was unknown, which fit best to the clinical focus hypothesis. One-second EEG epochs centred on the peak of the marked IED were filtered in the interval [1–70] Hz with a 4th-order Butterworth filter to avoid phase distortion, plus notch filtering at 50 Hz. EEG epochs that contained any artefacts surrounding the IED were discarded by visual inspection. IED epochs were averaged using the Cartool software (version 3.80) (Michel and Brunet, 2019) and spatially down-sampled to 219, 204, or 156 channels using MATLAB R2016a (The MathWorks, Inc., Natick, US-MA). The 257- and 219-channel setups included all 6 inferior temporal electrodes of the IFCN 25-channel array while the 204-channel setup included P9/P10 only, and all six were removed for the 156-channel setup (Fig. 1 A, Supplementary Fig. 1). Using Cartool, channels corrupted by continuous artefacts were identified via visual inspection of both EEG waveforms and surface voltage maps and corrected via interpolation from nearby channels using 3D splines. Finally, IED epochs were temporally down-sampled to 250 Hz.

2.3. MRI acquisition and pre-processing

Each patient's individual structural T1 or MPRAGE MRI image, acquired during pre-surgical evaluation, was re-sampled to 1 mm^3 isotropic resolution using cubic interpolation and pre-processed with Freesurfer (version 6.0.1) (Reuter et al., 2012) and the Connectome Mapper 3 open-source pre-processing software (Tourbier et al., 2019). A grey matter mask was generated which excluded brainstem and cerebellum. Based on the Desikan-Killiany anatomical atlas (Desikan et al., 2006; Destrieux et al., 2010), the grey matter was then parcelled into 82 regions of interest (41 per hemisphere) which were again grouped into 38 "sublobar" areas (19 per hemisphere; Supplementary Table 1).

2.4. Forward models

With the use of Cartool and based on fiducial points at the head surface, the average 257-channel array was interactively co-

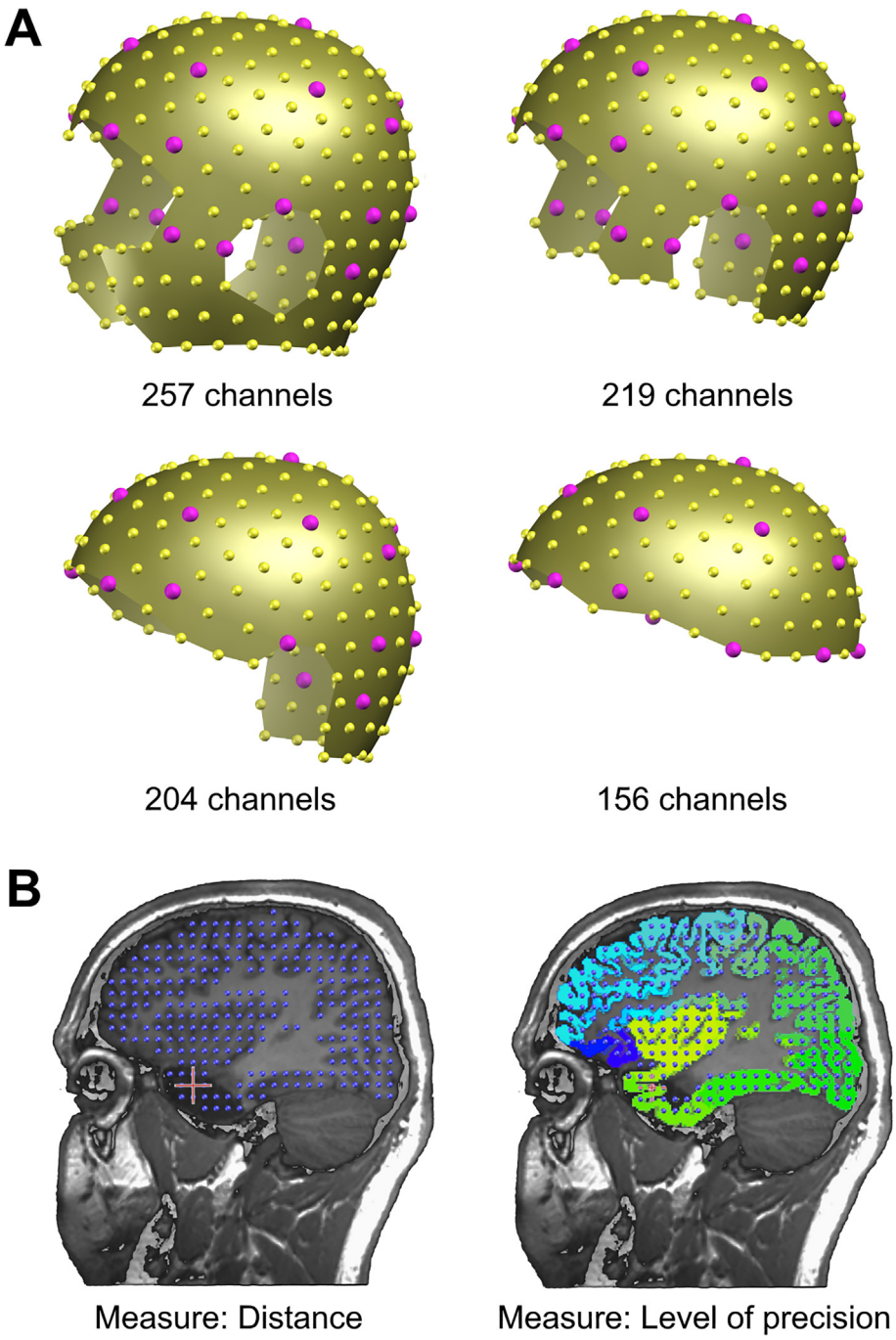

Fig. 1. A, High-density EEG arrays with 257 channels, down-sampled to 219 channels, 204 channels, and 156 channels, in 3D view. For comparison, electrodes included in the 25-channel array recommended by the International Federation of Clinical Neurophysiology (IFCN) (Seeck et al., 2017) are given in pink. Please note that the high-density electrode array does not perfectly match the IFCN 25-channel array. - B, Example of the maximum source localising inside the resection cavity (left) and, thus, in a sublobe overlapping with by the resection (right).

registered to the patient's individual 3D-MRI. Using MATLAB, this co-registered array was down-sampled to 219-, 204- and 156-electrode setups, respectively. For the forward solution, a simplified realistic 3-shell head model was used with consideration of age-adjusted skull thickness (Locally Spherical Model with Anatomical Constraints; LSMAC) (Michel and Brunet, 2019). For ESI of IEDs, the LSMAC was found to yield as accurate results as more sophisticated head models, namely the Boundary Element Model and the Finite Element Model (Birot et al., 2014). A grid of around 5000 sources was distributed equally throughout the grey matter mask. This grid was kept unmodified for all electrode setups to allow for comparison of localisations. Both the lead-field matrix and the inverse matrix were computed independently for each electrode setup.

2.5. Source localisation

The inverse solution was calculated using LAURA (Local Autoregressive Average), one of the state-of-the-art techniques of distributed inverse solutions which attempts to impose reliable biophysical and physiological constraints on the minimum norm algorithm (Grave-de Peralta et al., 2004). The patient's postsurgical MRI or computed tomography (CT) scan was resliced using SPM8 (Wellcome Centre for Human Neuroimaging, University College Lon-

don, UK) and co-registered to the grid of solution points. Since we did not use any covariance matrix to correct for noise, ESI could be robustly performed at every single time point. The IED's rising phase could be as short as 20 ms (Appendix 2), so we based the evaluation on predefined time points and not on changes in the scalp voltage map. The source of maximum amplitude at 50% of the IED's rising slope (by default; or alternatively at 10%, 25%, 75%, or the peak) was identified and visually compared to the resected brain area.

2.6. Assessment of concordance

Two separate measures of concordance were applied.

- Distance: The shortest spatial distance in one of the 3 orthogonal planes (axial, sagittal, coronal) between the maximum source and the edge of the resection was assessed. If the maximum source was located within the resection cavity, the distance was considered 0 mm; otherwise distance was classified as <10 mm, <20 mm or >20 mm from the border of resection. Distances of 0–10 mm were considered concordant to the resected brain area (Fig. 1 B).
- Level of precision: According to the parcellation of the grey matter, the maximum source was compared to sublobes, lobe (s), and hemisphere affected by the surgery (Fig. 1 B). Here, sublobar precision was considered concordant.

To estimate the quality of the results, concordance in favourable outcome patients (ILAE 1 + 2) was considered true positive (TP), and discordance in unfavourable outcome patients (ILAE 3–5) was considered true negative (TN). Accordingly, concordance in unfavourable outcome was considered false positive (FP), and discordance in favourable outcome was considered false negative (FN). Sensitivity was calculated as TP/(TP + FN), and specificity as TN/(TN + FP). Overall accuracy was calculated as (TP + TN)/(TP + TN + FP + FN). The diagnostic odds ratio (OR) of favourable post-surgical outcome in case of concordant *vs.* discordant ESI results was calculated as (TP*TN)/(FP*FN) (Sharma et al., 2019). Please note that this approach has a limitation: Unfavourable seizure outcome does not reliably prove incorrect estimation of the epileptogenic zone, and neither does discordant ESI in such a case imply that the ESI maximum lies in the true epileptogenic zone (outside the resection). Thus, the definitions of TN and specificity are less reliable than the definitions of TP and sensitivity (Rikir et al., 2017).

2.7. Statistics

Statistical analyses were performed using SPSS 25 (IBM, Armonk, US-NY). Data are given as percent or as median and interquartile range (IQR). ESI accuracies obtained with a specific methodology (referring to electrode setup and time point) were compared intra-individually and pairwise to that achieved with the default methodology (204 channels, 50% of the IED's rising phase) using Wilcoxon test. Mann-Whitney U test was used for comparisons across patients. A value of $p < 0.05$ was considered statistically significant. All p-values given in this manuscript were corrected for multiple comparisons according to the Benjamini-Hochberg procedure, assuming a false discovery rate of 0.05 (Hemmerich, 2016). Graphs were created using SigmaPlot 14 (Systat Software Inc., San José, US-CA).

3. Results

3.1. Patient characteristics

Among 304 subjects screened, 45 patients operated between October 2007 and April 2018 fulfilled the inclusion criteria for this study (Supplementary Fig. 2). Thirty-one of these were female (69%), the median age at onset of epilepsy was 8 years (IQR 2–16, range 0–27), and the median age at surgery was 18 years (IQR 13–32, range 7–53). Eighteen patients had extratemporal resections (40%) while the remaining 27 had a resection restricted to the (anterior) temporal lobe (60%; Fig. 2 A). One patient (#44, ILAE 5) had a frontobasal resection. Resections were left-sided in 28 subjects (62%), no patient had bilateral surgery. Regarding 12-month post-surgical outcome, 28, 2, 6, 7 and 2 patients (62%, 4%, 13%, 16%, and 4%), were classified as ILAE 1, 2, 3, 4 and 5, respectively. No patient had an outcome of ILAE class 6. Among the 18 subjects with extratemporal resections, 11 (61%) had a favourable 12-month outcome (ILAE 1 + 2), compared to 19 (70%) out of the 27 subjects with a temporal resection. For detailed information on the individual patients, please see Appendix 2.

3.2. Average IEDs and artefacted channels

Depending on the duration of the high-density EEG recording and on the individual patient, the number of homologous IEDs ranged from 3-269 with a median of 27 (IQR 18–38; Appendix 2). For 16 patients, only the IED average was available in the database, and the number of averaged spikes could retrospectively not be ascertained. It was not possible to retrospectively determine electrode impedance values throughout the EEG recordings. For the default 204-channel array, a median of 1 channel (IQR 0–4) was visually considered artefact-ridden and required interpolation, representing 0.5% of all channels. By comparison, the median of corrupted channels was 6 for the original 257-channel array (IQR 1–13; 2.3%; $p = 0.001$), 3 for 219 channels (IQR 0–7; 1.4%; $p = 0.018$), and again 1 for 156 channels (IQR 0–4; 0.6%; $p = 0.97$; Appendix 2).

3.3. ESI with 204 channels at half-rise of IED

Using the "default method", the maximum source was located inside the resection cavity in 19 patients (42%) and less than 10 mm remote from its edge in another 9 patients (20%), yielding an overall concordance of 62% in terms of distance (Fig. 2). Regarding the levels of precision, in 32 patients (71%) the maximum source was located inside a sublobe affected by the surgery (i.e., concordant), and outside the sublobes but within the affected lobe(s) in another 3 patients (7%).

In patients with favourable vs. unfavourable post-surgical outcome, 67% vs. 53% had a distance of 0–10 mm between ESI maximum and resection edge, and 50% vs. 27% had the ESI maximum inside the resection ($p = 0.24$ across all distance levels). Sublobar precision was achieved in 83% vs. 47% ($p = 0.042$). This means, sensitivities of ESI were 67% (distance 0–10 mm) and 83% (sublobar precision). Specificities were 47% and 54%, respectively, and overall accuracies were 60% and 73% (Table 1). ORs for favourable outcome (ILAE 1 + 2) were 1.8 in case of 0–10 mm distances between maximum source and resection, 2.8 in case of localisation within the resection (0 mm only), and 5.7 in case of sublobar concordance. ESI was significantly more sensitive in subjects with a temporal resection (79% with 0–10 mm distance and 100% with sublobar precision) than in those with extratemporal resections (45%, $p = 0.002$, and 54%, $p < 0.001$; Fig. 2 A, Fig. 3 B-C).

Overall accuracies were similar in patients with unknown vs. known numbers of IEDs to be averaged (distance: 59% vs. 63%; level of precision: 72 vs. 75%; Supplementary Table 3 and Appendix 2). Descriptively, ESI was not more accurate in case of very large resections (e.g., patients #1 and #5) than in case of smaller resections (e.g., patients #10–27). In those 8 patients with more than one cluster of IEDs, ESI based on another IED type did not lead to more concordant results (data not shown). When levels of Tikho-

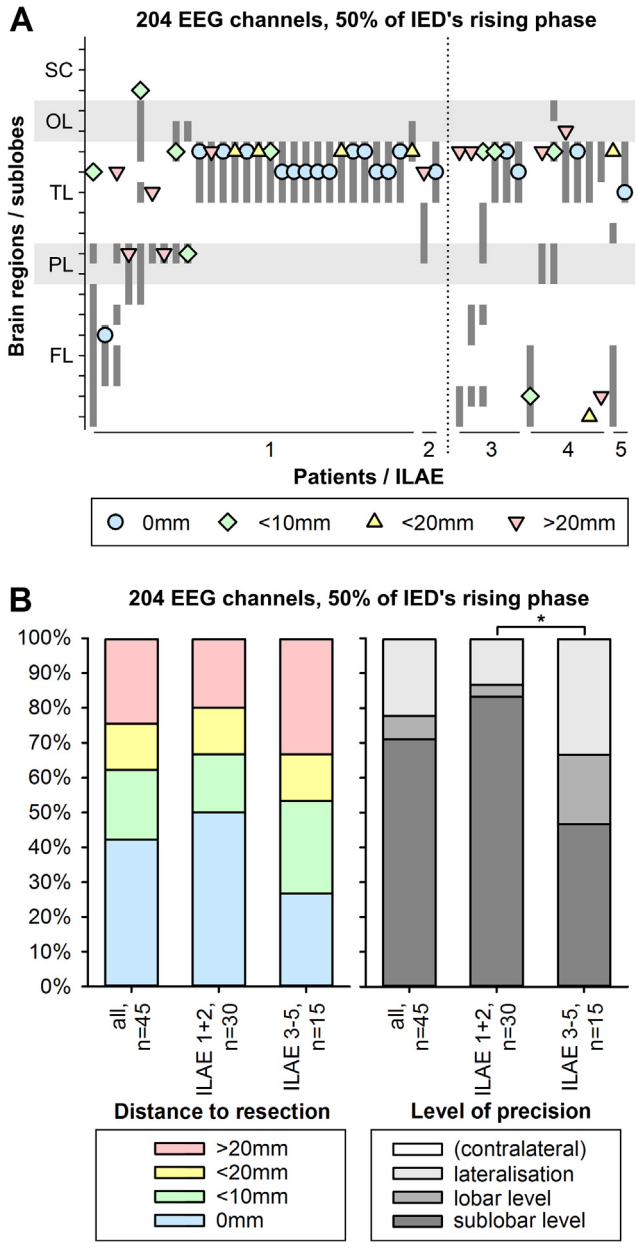

Fig. 2. A, individual electric source imaging (ESI) results obtained with the "default method" of 204 EEG channels, measured at 50% of the averaged interictal epileptic discharge's (IED's) rising phase. X-axis: Individual patients, sorted by 12-month outcome according to the International League Against Epilepsy (ILAE) classification (Wieser et al., 2001). Y-axis: ESI maximum (symbol) compared to brain areas affected by resection (grey bar), given on a sublobar level, sorted by brain regions. SC, subcortical grey matter; OL, occipital lobe; TL, temporal lobe; PL, parietal lobe; FL, frontal lobe. Symbols indicate distances between ESI maximum and resected brain area: blue circle, 0 mm; green rhombus, <10 mm; yellow upward triangle, <20 mm; red downward triangle, >20 mm. B, overview on distances between maximum source and resected brain area (left, coloured bars) and levels of precision (right, greyscale bars), each given for all 45 patients, those 30 with favourable 12-month outcome only, and those 15 with rather unfavourable outcome (left to right). *, $p < 0.05$.

nov regularization were changed manually (Michel and Brunet, 2019), ESI results did not change either (data not shown).

3.4. Different electrode setups

Individual ESI maxima gradually varied between the different electrode setups tested (Supplementary Fig. 3). In comparison to the default 204-channel setup, overall accuracies and diagnostic ORs decreased when other electrode setups were applied (Supplementary Table 2). When only patients with favourable postsurgical outcome were assessed (ILAE 1 + 2, n = 30), results obtained with 257 electrodes were significantly less precise than those based on 204 channels (sublobar precision: 57% vs. 83%, $p = 0.042$; Fig. 3). Otherwise, differences were statistically not significant, but the default 204-channel approach tended to perform best.

Table 1
Overall statistics on ESI results, achieved with the default method.

	ESI measure: distance 0–10 mm	ESI measure: sublobar precision
Concordance, all patients (positives, P)	62% (28/45)	71% (32/45)
Concordance, extratemporal resections (P)	44% (8/18)	44% (8/18)
Concordance, temporal resection (P)	74% (20/27)	89% (24/27)
Concordance, ILAE 1 + 2 (TP)	67% (20/30)	83% (25/30)
Concordance, ILAE 3–5 (FP)	53% (8/15)	47% (7/15)
Sensitivity, all patients	67%	83%
Sensitivity, extratemporal resections	46%	55%
Sensitivity, temporal resection	79%	100%
Specificity, all patients	47%	54%
Specificity, extratemporal resections	57%	71%
Specificity, temporal resection	38%	38%
Overall accuracy, all patients	60%	73%
Overall accuracy, extratemporal resections	50%	61%
Overall accuracy, temporal resection	67%	82%
Diagnostic OR, all patients	1.8	5.7
Diagnostic OR, extratemporal resections	1.1	3.0
Diagnostic OR, temporal resection	2.3	∞

Electric source imaging (ESI) concordances, sensitivities, specificities, overall accuracies, and diagnostic odds ratios for all patients and subgroups, respectively, estimated in distance between ESI maximum and resection, and in sublobar concordance. ILAE, International League Against Epilepsy surgical outcome classification (Wieser et al., 2001). TP, true positives. FP, false positives. OR, odds ratio.

3.5. Different time points across the IED's rising phase

Time points different from 50% of the IED's rising slope did not improve ESI concordances. At 10% of the IED's rising phase, accuracy was even below 50% with 23% of ESI maxima in the hemisphere contralateral to the resection ($p < 0.05$; Fig. 4). Results at 25%, 75% and at the IED peak were not significantly different from the default approach at 50%.

4. Discussion

In our study, ESI did not perform better if information from caudal EEG channels over cheeks and necks was included. In both extratemporal and temporal lobe epilepsy, the reduced 204-channel setup tended to yield the most accurate ESI results for patients who underwent successful epilepsy surgery. To our knowledge, this is the first study to show that increasing the numbers of EEG electrodes beyond 204 channels and below the recommended "9/10" lines of the 10/10 international system (Seeck et al., 2017) does not necessarily improve the precision of ESI.

Using our default approach of 204 EEG channels and 50% of the IED's rising slope, ESI achieved accuracies of 60–73% and diagnostic ORs of 1.8–5.7. This is in the range of previous studies, although it

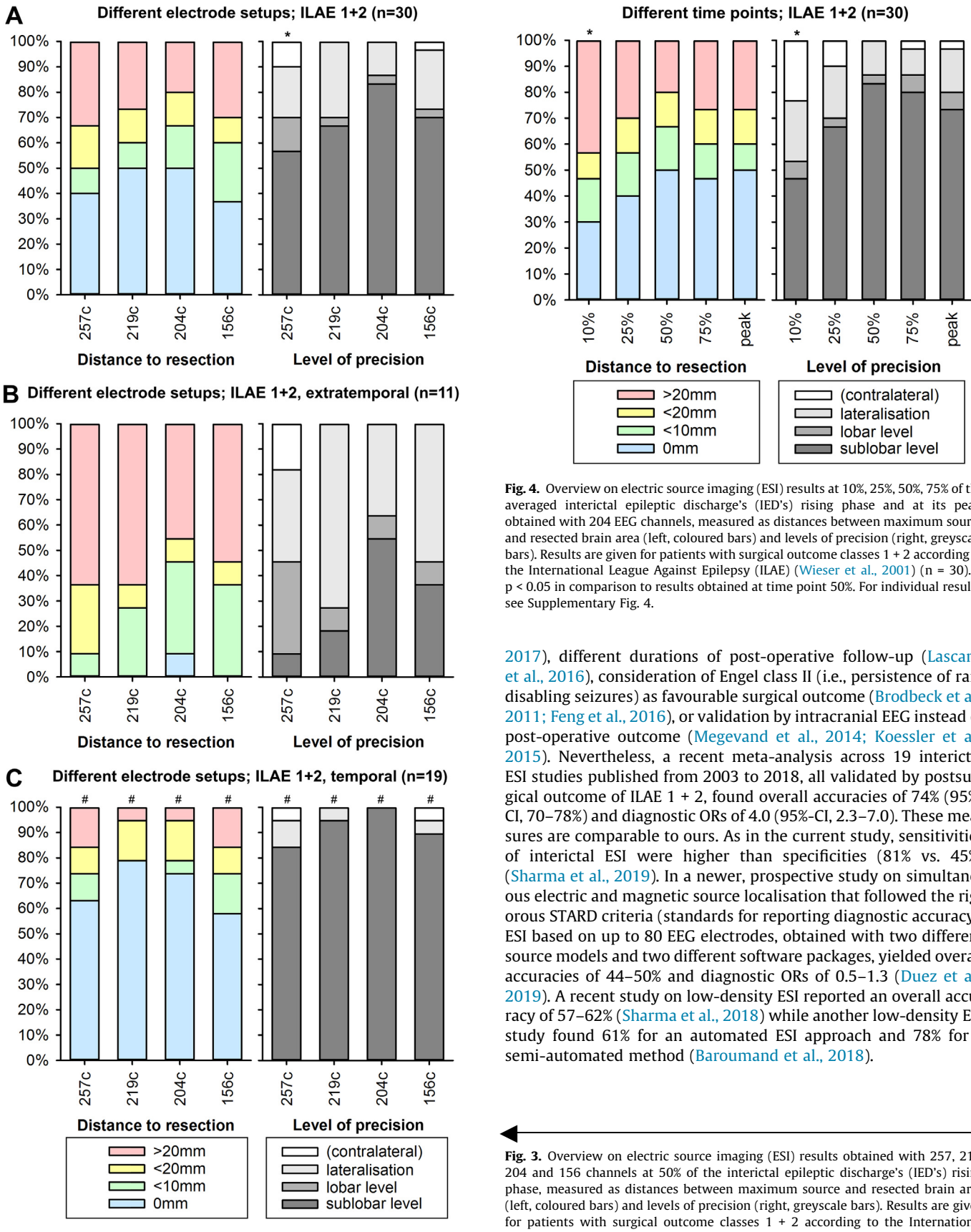

Fig. 4. Overview on electric source imaging (ESI) results at 10%, 25%, 50%, 75% of the averaged interictal epileptic discharge's (IED's) rising phase and at its peak, obtained with 204 EEG channels, measured as distances between maximum source and resected brain area (left, coloured bars) and levels of precision (right, greyscale bars). Results are given for patients with surgical outcome classes 1 + 2 according to the International League Against Epilepsy (ILAE) (Wieser et al., 2001) (n = 30). *, $p < 0.05$ in comparison to results obtained at time point 50%. For individual results, see Supplementary Fig. 4.

is difficult to formally compare these quality measures to other studies on interictal ESI, because of different methodological approaches, e.g., different sublobar parcellations (Centeno et al., 2017), different durations of post-operative follow-up (Lascano et al., 2016), consideration of Engel class II (i.e., persistence of rare disabling seizures) as favourable surgical outcome (Brodbeck et al., 2011; Feng et al., 2016), or validation by intracranial EEG instead of post-operative outcome (Megevand et al., 2014; Koessler et al., 2015). Nevertheless, a recent meta-analysis across 19 interictal ESI studies published from 2003 to 2018, all validated by postsurgical outcome of ILAE 1 + 2, found overall accuracies of 74% (95%-CI, 70–78%) and diagnostic ORs of 4.0 (95%-CI, 2.3–7.0). These measures are comparable to ours. As in the current study, sensitivities of interictal ESI were higher than specificities (81% vs. 45%) (Sharma et al., 2019). In a newer, prospective study on simultaneous electric and magnetic source localisation that followed the rigorous STARD criteria (standards for reporting diagnostic accuracy), ESI based on up to 80 EEG electrodes, obtained with two different source models and two different software packages, yielded overall accuracies of 44–50% and diagnostic ORs of 0.5–1.3 (Duez et al., 2019). A recent study on low-density ESI reported an overall accuracy of 57–62% (Sharma et al., 2018) while another low-density ESI study found 61% for an automated ESI approach and 78% for a semi-automated method (Baroumand et al., 2018).

Fig. 3. Overview on electric source imaging (ESI) results obtained with 257, 219, 204 and 156 channels at 50% of the interictal epileptic discharge's (IED's) rising phase, measured as distances between maximum source and resected brain area (left, coloured bars) and levels of precision (right, greyscale bars). Results are given for patients with surgical outcome classes 1 + 2 according to the International League Against Epilepsy (ILAE) (Wieser et al., 2001) (A), those 11 with extratemporal resections (B), and those 19 with temporal resections only (C). *, $p < 0.05$ in comparison to results obtained with 204 EEG channels. #, $p < 0.05$ between extratemporally and temporally resected cases (B vs. C). For individual results, see Supplementary Fig. 3.

As expected, in the current study, caudal EEG channels were prone to artefacts. The percentage of corrupted channels was highest in the full 257-channel setup (median: 2.3%; maximum: 11%). Information from these artefacted channels had to be interpolated from their neighbours, as long as the neighbouring channels were not subject to interpolation themselves. Manual identification of artefacted channels costs working time that could be saved through down-sampling of the electrode setups. Apart from EEG artefacts, cheek and neck electrodes are located on muscles and conjunctive tissue but remote from the brain. Eyeballs, air cavities of sinuses, nose and mouth as well as the holes of the skull base are challenges for the head model (Montes-Restrepo et al., 2014). These circumstances make it difficult for a three-shell forward model like LSMAC to properly reproduce the volume conduction to caudal electrodes, what is likely to be another reason for lower ESI accuracy in the 257-channel setup.

Interestingly, in the meta-analysis cited above, high-density ESI (i.e., 64–257 EEG channels) had virtually the same accuracy as low-density ESI (19–32 channels) although patients populations were not detailed in both groups, particularly with respect to proportions of temporal lobe epilepsy and extratemporal epilepsy (Sharma et al., 2019). In the light of our current findings, it seems possible that for ESI based on the full 128- and 257-channel setups, the advantages of high electrode density were counterbalanced by inaccurate signal recording and processing from very caudal face and neck electrodes. On the other hand, inferior temporal and occipital regions do need to be covered for ESI, since our 156-channel array located above the hat brim line also led to less accurate results than the 204-channel setting. Thus, a relocation of high-density EEG electrodes from cheeks and neck towards the scalp, leading to smaller interelectrode distances within the borders of the 204- or 219-channel setup, could improve ESI accuracy.

As a limitation of our study, there were no cases with fronto- or occipito-basal epilepsy and favourable surgery outcome. Thus, to compare epileptic activity in basal structures vs. the convexity, we relied on the comparison of temporal to extratemporal cases. ESI in temporal lobe epilepsy had higher sensitivities (79–100% vs. 46–55%), overall accuracies (67–82% vs. 50–61%) and ORs for favourable outcome (2.3-∞ vs. 1.1–3.0) than in extratemporal epilepsy, but lower specificities (38% vs. 57–71%; Table 1, Fig. 3 BC). This was already the case in some previous studies (Brodbeck et al., 2011; Coutin-Churchman et al., 2012; van Mierlo et al., 2017; Toscano et al., 2020) but not in others (Megevand et al., 2014; Abdallah et al., 2017). In an earlier work on interictal low-density ESI in children, accuracy was markedly higher in extratemporal vs. temporal lobe epilepsy (Sperli et al., 2006). The authors argued that in temporal lobe epilepsy, a lack of inferior temporal EEG electrodes led to a shift of ESI maxima from basal temporal to extratemporal sources. In our current study, this shift seems reversed: Inclusion of very caudal electrodes as in the 257- and the 219-channel setup led to a shift of ESI maxima towards the temporal lobes even in extratemporal epilepsy (Supplementary Fig. 3). However, the accuracy of ESI in extratemporal epilepsies has only been assessed in small stand-alone studies or as a small subset of patients in larger clinical cohorts that mostly included temporal cases. Thus, the yield of ESI in extratemporal epilepsies needs to be better assessed in a larger study.

In a recent ESI study based on automatically detected IEDs, most accurate results were found at the IED peak (van Mierlo et al., 2017). This was most likely attributable to an optimal signal-to-noise ratio at that time point, since IEDs were centred around the peak for averaging. Although we did the same, ESI accuracy in our study decreased at time points later than 50% of the IED's rising phase. The most likely explanation for this is propagation: During the time course of an IED's upswing, the source of maximum activity can move away from the IED origin (Merlet et al., 1997; Lantz et al., 2003b; Bast et al., 2006; Plummer et al., 2010).

Consistent with this, another recent article on electric and magnetic source localisation reported best results at very early time points of IEDs (Plummer et al., 2019). In our study again, earlier time points than 50% yielded less accuracy. In a quarter of successfully operated patients, source maxima at 10% of the IED's rising phase were even contralateral to the resection (Fig. 4, Supplementary Fig. 4). This points to a relatively high instability of the source at IED onset where the signal-to-noise ratio is well-known to be low (Bast et al., 2006; Ray et al., 2007; Wennberg and Cheyne, 2014). The discrepancy between the two articles may be due to a higher overall signal-to-noise ratio in the other study: There was a 3-times higher number of IEDs per average (median: 76) than in ours (median: 27). In addition, IEDs were described as "relatively complex with polyphasic components preceding a dominant negative-peak". This suggests a high signal-to-noise ratio already at early time points of the IED, compared to rather simple, biphasic spikes or sharp waves in our data. In our case, 50% of the IEDs rising phase seemed an optimal compromise between little source propagation (early stages) and high signal-to-noise ratio (towards the peak). In general, selection of the time point may have to be adapted to the number of IEDs per average and to the IED morphology which both affect the signal-to-noise ratio.

At least for low-density ESI, a minimum of 8–25 single IEDs have been recommended for IED averaging to yield acceptable signal-to-noise ratios and both reliable and valid localisation results (Bast et al., 2006; Wennberg and Cheyne, 2014). Unfortunately, six patients of our study cohort had less than 10 IEDs to be averaged, and the number of IEDs could retrospectively not be ascertained in another 16 patients. Still, ESI in these specific cases was as accurate as in the other patients with more than 10 IEDs (Supplementary Fig. 5).

For our study, we used a methodology that is easy to handle and, thus, most feasible in clinical routine: We took averaged IEDs and a simplified realistic 3-shell head model, and we considered the spatial ESI maximum within a distributed inverse solution at one specific time point. We welcome future studies to replicate our findings using different methodological approaches, e.g. more sophisticated head models, single dipole inverse solutions, and/or ictal EEG. For our approach, we can conclude that adding information from caudal EEG electrodes over cheeks and neck does not necessarily improve accuracy of high-density ESI, most likely because of both higher artefact load and suboptimal biophysical modelling for the lower skull structures.

Declaration of Competing Interest

M. Seeck and S. Vulliemoz are shareholders and advisors of Epilog NV (Ghent, BE). M. Seeck received speaker's fees from Philips and Desitin. All other authors have no conflicts of interest to report.

Acknowledgements

This study was funded by the German Research Foundation (DFG 422589384 to B. Vorderwülbecke) and the Swiss National Science Foundation (SNSF 163398 and Sinergia 180365 to M. Seeck; SNSF 169198, 192749, and CRSII5 170873 to S. Vulliemoz). The funders were not involved in the study design, in the collection, analysis and interpretation of data, in the writing of the report, or in the decision to submit the article for publication. – The authors wish to thank Christian Korff MD, Shahan Momjian MD, and Karl Schaller MD for their work with the patients evaluated and operated for this study, and Amir Baroumand PhD, Göran Lantz MD PhD, Pierre

Mégevand MD PhD, Christoph M. Michel PhD, and Pieter van Mierlo PhD for valuable discussions and feedback.

Author contributions

M. Carboni and S. Vulliemoz designed the study. B. Vorderwülbecke, M. Carboni, L. Spinelli, M. Seeck and S. Vulliemoz acquired the data. B. Vorderwülbecke, M. Carboni, S. Tourbier, D. Brunet and M. Seeber processed the data. B. Vorderwülbecke performed the statistical analyses and drafted the manuscript. All authors critically reviewed the manuscript and approved the final version to be published.

Appendix A. Supplementary material

Supplementary data to this article can be found online at https://doi.org/10.1016/j.clinph.2020.09.018.

References

Abdallah C, Maillard LG, Rikir E, Jonas J, Thiriaux A, Gavaret M, et al. Localizing value of electrical source imaging: Frontal lobe, malformations of cortical development and negative MRI related epilepsies are the best candidates. Neuroimage Clin 2017;16:319–29. https://doi.org/10.1016/j.nicl.2017.08.009 [doi];S2213-1582(17)30199-7 [pii].

Baroumand AG, van Mierlo P, Strobbe G, Pinborg LH, Fabricius M, Rubboli G, et al. Automated EEG source imaging: a retrospective, blinded clinical validation study. Clin Neurophysiol 2018;129:2403–10. https://doi.org/10.1016/j.clinph.2018.09.015.

Bast T, Boppel T, Rupp A, Harting I, Hoechstetter K, Fauser S, et al. Noninvasive source localization of interictal EEG spikes: effects of signal-to-noise ratio and averaging. J Clin Neurophysiol 2006;23(6):487–97. https://doi.org/10.1097/01.wnp.0000232208.14060.c7.

Beniczky S, Rosenzweig I, Scherg M, Jordanov T, Lanfer B, Lantz G, et al. Ictal EEG source imaging in presurgical evaluation: high agreement between analysis methods. Seizure 2016;43:1–5. https://doi.org/10.1016/j.seizure.2016.09.017.

Birot G, Spinelli L, Vulliemoz S, Megevand P, Brunet D, Seeck M, et al. Head model and electrical source imaging: a study of 38 epileptic patients. Neuroimage Clin 2014;5:77–83. https://doi.org/10.1016/j.nicl.2014.06.005 [doi];S2213-1582(14)00081-3 [pii].

Brodbeck V, Spinelli L, Lascano AM, Wissmeier M, Vargas MI, Vulliemoz S, et al. Electroencephalographic source imaging: a prospective study of 152 operated epileptic patients. Brain 2011;134:2887–97. awr243 [pii];10.1093/brain/awr243 [doi].

Centeno M, Tierney TM, Perani S, Shamshiri EA, St Pier K, Wilkinson C, et al. Combined electroencephalography-functional magnetic resonance imaging and electrical source imaging improves localization of pediatric focal epilepsy. Ann Neurol 2017;82(2):278–87. https://doi.org/10.1002/ana.25003.

Coutin-Churchman PE, Wu JY, Chen LL, Shattuck K, Dewar S, Nuwer MR. Quantification and localization of EEG interictal spike activity in patients with surgically removed epileptogenic foci. Clin Neurophysiol 2012;123(3):471–85. https://doi.org/10.1016/j.clinph.2011.08.007.

Desikan RS, Segonne F, Fischl B, Quinn BT, Dickerson BC, Blacker D, et al. An automated labeling system for subdividing the human cerebral cortex on MRI scans into gyral based regions of interest. Neuroimage 2006;31(3):968–80. https://doi.org/10.1016/j.neuroimage.2006.01.021. S1053-8119(06)00043-7 [pii].

Destrieux C, Fischl B, Dale A, Halgren E. Automatic parcellation of human cortical gyri and sulci using standard anatomical nomenclature. Neuroimage 2010;53(1):1–15. https://doi.org/10.1016/j.neuroimage.2010.06.010. S1053-8119(10)00854-2 [pii].

Duez L, Tankisi H, Hansen PO, Sidenius P, Sabers A, Pinborg LH, et al. Electromagnetic source imaging in presurgical workup of patients with epilepsy: a prospective study. Neurology 2019;92(6):e576–86. https://doi.org/10.1212/WNL.0000000000006877.

Feng R, Hu J, Pan L, Wu J, Lang L, Jiang S, et al. Application of 256-channel dense array electroencephalographic source imaging in presurgical workup of temporal lobe epilepsy. Clin Neurophysiol 2016;127(1):108–16. https://doi.org/10.1016/j.clinph.2015.03.009.

Foged MT, Martens T, Pinborg LH, Hamrouni N, Litman M, Rubboli G, et al. Diagnostic added value of electrical source imaging in presurgical evaluation of patients with epilepsy: a prospective study. Clin Neurophysiol 2020;131(1):324–9. https://doi.org/10.1016/j.clinph.2019.07.031.

Grave-de Peralta R, Gonzalez-Andino S, Gomez-Gonzalez CM. The biophysical foundations of the localisation of encephalogram generators in the brain. The application of a distribution-type model to the localisation of epileptic foci. Rev Neurol 2004;39(8):748–56.

Hemmerich W. Rechner zur Adjustierung des α-Niveaus: StatistikGuru, https://statistikguru.de/rechner/adjustierung-des-alphaniveaus.html; 2016 [Accessed 19.03.2020].

Koessler L, Cecchin T, Colnat-Coulbois S, Vignal JP, Jonas J, Vespignani H, et al. Catching the invisible: mesial temporal source contribution to simultaneous EEG and SEEG recordings. Brain Topogr 2015;28(1):5–20. https://doi.org/10.1007/s10548-014-0417-z.

Lantz G, Grave de Peralta R, Spinelli L, Seeck M, Michel CM. Epileptic source localization with high density EEG: how many electrodes are needed?. Clin Neurophysiol 2003a;114(1):63–9. https://doi.org/10.1016/S1388-2457(02)00337-1.

Lantz G, Spinelli L, Seeck M, de Peralta Menendez RG, Sottas CC, Michel CM. Propagation of interictal epileptiform activity can lead to erroneous source localizations: a 128-channel EEG mapping study. J Clin Neurophysiol 2003b;20(5):311–9.

Lascano AM, Perneger T, Vulliemoz S, Spinelli L, Garibotto V, Korff CM, et al. Yield of MRI, high-density electric source imaging (HD-ESI), SPECT and PET in epilepsy surgery candidates. Clin Neurophysiol 2016;127(1):150–5. https://doi.org/10.1016/j.clinph.2015.03.025. S1388-2457(15)00314-4 [pii].

Megevand P, Spinelli L, Genetti M, Brodbeck V, Momjian S, Schaller K, et al. Electric source imaging of interictal activity accurately localises the seizure onset zone. J Neurol Neurosurg Psychiatry 2014;85(1):38–43. https://doi.org/10.1136/jnnp-2013-305515.

Merlet I, Paetau R, Garcia-Larrea L, Uutela K, Granstrom ML, Mauguiere F. Apparent asynchrony between interictal electric and magnetic spikes. Neuroreport 1997;8(5):1071–6. https://doi.org/10.1097/00001756-199703240-00002.

Michel CM, Brunet D. EEG source imaging: a practical review of the analysis steps. Front Neurol 2019;10:325. https://doi.org/10.3389/fneur.2019.00325.

Montes-Restrepo V, van Mierlo P, Strobbe G, Staelens S, Vandenberghe S, Hallez H. Influence of skull modeling approaches on EEG source localization. Brain Topogr 2014;27(1):95–111. https://doi.org/10.1007/s10548-013-0313-y.

Nemtsas P, Birot G, Pittau F, Michel CM, Schaller K, Vulliemoz S, et al. Source localization of ictal epileptic activity based on high-density scalp EEG data. Epilepsia 2017;58(6):1027–36. https://doi.org/10.1111/epi.13749.

Pittau F, Grouiller F, Spinelli L, Seeck M, Michel CM, Vulliemoz S. The role of functional neuroimaging in pre-surgical epilepsy evaluation. Front Neurol 2014;5:31. https://doi.org/10.3389/fneur.2014.00031.

Plummer C, Vogrin SJ, Woods WP, Murphy MA, Cook MJ, Liley DTJ. Interictal and ictal source localization for epilepsy surgery using high-density EEG with MEG: a prospective long-term study. Brain 2019;142(4):932–51. https://doi.org/10.1093/brain/awz015.

Plummer C, Wagner M, Fuchs M, Harvey AS, Cook MJ. Dipole versus distributed EEG source localization for single versus averaged spikes in focal epilepsy. J Clin Neurophysiol 2010;27(3):141–62. https://doi.org/10.1097/WNP.0b013e3181dd5004.

Ray A, Tao JX, Hawes-Ebersole SM, Ebersole JS. Localizing value of scalp EEG spikes: a simultaneous scalp and intracranial study. Clin Neurophysiol 2007;118(1):69–79. https://doi.org/10.1016/j.clinph.2006.09.010.

Reuter M, Schmansky NJ, Rosas HD, Fischl B. Within-subject template estimation for unbiased longitudinal image analysis. Neuroimage 2012;61(4):1402–18. https://doi.org/10.1016/j.neuroimage.2012.02.084.

Rikir E, Koessler L, Ramantani G, Maillard LG. Added value and limitations of electrical source localization. Epilepsia 2017;58(1):174–5. https://doi.org/10.1111/epi.13643.

Seeck M, Koessler L, Bast T, Leijten F, Michel C, Baumgartner C, et al. The standardized EEG electrode array of the IFCN. Clin Neurophysiol 2017;128(10):2070–7. https://doi.org/10.1016/j.clinph.2017.06.254.

Sharma P, Scherg M, Pinborg LH, Fabricius M, Rubboli G, Pedersen B, et al. Ictal and interictal electric source imaging in pre-surgical evaluation: a prospective study. Eur J Neurol 2018;25(9):1154–60. https://doi.org/10.1111/ene.13676.

Sharma P, Seeck M, Beniczky S. Accuracy of Interictal and Ictal electric and magnetic source imaging: a systematic review and meta-analysis. Front Neurol 2019;10:1250. https://doi.org/10.3389/fneur.2019.01250.

Song J, Davey C, Poulsen C, Luu P, Turovets S, Anderson E, et al. EEG source localization: sensor density and head surface coverage. J Neurosci Methods 2015;256:9–21. https://doi.org/10.1016/j.jneumeth.2015.08.015.

Sperli F, Spinelli L, Seeck M, Kurian M, Michel CM, Lantz G. EEG source imaging in pediatric epilepsy surgery: a new perspective in presurgical workup. Epilepsia 2006;47(6):981–90. https://doi.org/10.1111/j.1528-1167.2006.00550.x.

Staljanssens W, Strobbe G, Holen RV, Birot G, Gschwind M, Seeck M, et al. Seizure onset zone localization from Ictal high-density EEG in refractory focal epilepsy. Brain Topogr 2017;30(2):257–71.

Toscano G, Carboni M, Rubega M, Spinelli L, Pittau F, Bartoli A, et al. Visual analysis of high density EEG: as good as electrical source imaging?. Clin Neurophysiol Pract 2020;5:16–22. https://doi.org/10.1016/j.cnp.2019.09.002.

Tourbier S, Aleman-Gomez Y, Griffa A, Hagmann P. connectomicslab/connectomemapper3: connectome Mapper v3.0.0-beta-20190815. Zenodo 2019.

van Mierlo P, Strobbe G, Keereman V, Birot G, Gadeyne S, Gschwind M, et al. Automated long-term EEG analysis to localize the epileptogenic zone. Epilepsia Open 2017;2(3):322–33. https://doi.org/10.1002/epi4.12066.

Wennberg R, Cheyne D. EEG source imaging of anterior temporal lobe spikes: validity and reliability. Clin Neurophysiol 2014;125(5):886–902. https://doi.org/10.1016/j.clinph.2013.09.042.

Wieser HG, Blume WT, Fish D, Goldensohn E, Hufnagel A, King D, et al. ILAE Commission Report. Proposal for a new classification of outcome with respect to epileptic seizures following epilepsy surgery. Epilepsia 2001;42(2):282–6.

Zijlmans M, Zweiphenning W, van Klink N. Changing concepts in presurgical assessment for epilepsy surgery. Nat Rev Neurol 2019;15(10):594–606. https://doi.org/10.1038/s41582-019-0224-y.